Available online at www.sciencedirect.com
SCIENCE DIRECT®
International Journal of Heat and Mass Transfer 48 (2005) 1840–1850
International Journal of HEAT and MASS TRANSFER
www.elsevier.com/locate/ijhmt

Free convection in a wavy cavity filled with a porous medium

Aydin Misirlioglu [a], A. Cihat Baytas [a], Ioan Pop [b,*]

[a] Istanbul Technical University, Faculty of Aeronautics and Astronautics, 34469 Maslak-Istanbul, Turkey
[b] University of Cluj, Faculty of Mathematics, R-3400 Cluj, CP 253, Romania

Received 15 October 2004

Abstract

The steady-state free convection inside a cavity made of two horizontal straight walls and two vertical bent-wavy walls and filled with a fluid-saturated porous medium is numerically investigated in the present paper. The wavy walls are assumed to follow a profile of cosine curve. The horizontal walls are kept adiabatic, while the bent-wavy walls are isothermal but kept at different temperatures. The Darcy and energy equations (in non-dimensional stream function and temperature formulation) are solved numerically using the Galerkin Finite Element Method (FEM). Flow and heat transfer characteristics (isothermal, streamlines and local and average Nusselt numbers) are investigated for some values of the Rayleigh number, cavity aspect ratio and surface waviness parameter. The present results are compared with those reported in the open literature for a square cavity with straight walls. It was found that these results are in excellent agreement.

Keywords: Porous media; Wavy cavity; Heat transfer; Computational

1. Introduction

Convective heat transfer in porous media has attracted the attention of engineers and scientists from many varying disciplines such as, chemical, civil, environmental, mechanical, aerospace, nuclear engineering, applied mathematicians, geothermal physics, food science, etc. To a large extent, this interest is stimulated by the fact that thermally driven flows in porous media are of considerable practical applications in the modern industry. It has given insight in the understanding dynamics of terrestrial heat flow through aquifer, hot fluid and ignition front displacements in reservoir engineering, heat exchange between soil and atmosphere, flow of moisture through porous industrial materials, heat exchangers with fluidized beds, fibre and granular insulation materials, packed-bed chemical reactors, oil recovery, ceramic processing and catalytic reactors, to name just a few applications. The fundamental importance of convective flow in porous media has been ascertained in the recent books by Ingham and Pop [1], Nield and Bejan [2], Vafai [3], Pop and Ingham [4], Bejan and Kraus [5], Ingham et al. [6] and Bejan et al. [7] appeared periodically in the literature.

The prediction of heat transfer from irregular surfaces is a topic of fundamental importance for some heat transfer devices, such as, flat plate solar collectors, flat plate condensers in refrigerators, double-wall thermal insulation, underground cable systems, electric machinery, cooling system of micro-electronic devices, natural

* Corresponding author. Tel.: +40 264 194315; fax: +40 264 591906.
E-mail address: popi@math.ubbcluj.ro (I. Pop).

0017-9310/$ - see front matter © 2005 Elsevier Ltd. All rights reserved.
doi:10.1016/j.ijheatmasstransfer.2004.12.005

Nomenclature

a	amplitude of the wave
A	aspect ratio
g	gravitational acceleration, m s^{-2}
K	permeability of the porous medium, m^2
k	thermal conductivity, W m^{-1} K^{-1}
L	cavity height, m
Nu	local Nusselt number
Nu_a	average Nusselt number
Ra	Rayleigh number for porous medium
S	the length of the bent-wall, m
t	dimensionless time
$\bar{t}$	time, s
T	fluid temperature, K
T_c	temperature of the cold bent-wall (left), K
T_h	temperature of the hot bent-wall (right), K
T_0	characteristic temperature of the fluid-saturated porous medium, K
u, v	dimensionless velocity components along x- and y-axes, respectively
$\bar{u}, \bar{v}$	velocity components along x- and y-axes, respectively, m s^{-1}
W	average width of the cavity, m
x, y	dimensionless Cartesian coordinates
$\bar{x}, \bar{y}$	Cartesian coordinates, m

Greek symbols

α_m	effective thermal diffusivity, m^2 s^{-1}
β	coefficient of thermal expansion, K^{-1}
ε	the prescribed error
θ	dimensionless temperature
λ	surface waviness
ρ	fluid density, kg m^{-3}
σ	ratio of composite material heat capacity to convective fluid heat capacity
v	kinematic viscosity, m^2 s^{-1}
ψ	dimensionless stream function

circulation in the atmosphere, the molten core of the Earth, etc. In addition, roughened surfaces could be used in the cooling of electrical and nuclear components where the wall heat flux is known. Surfaces are sometimes intentionally roughened to enhance heat transfer. Extensive studies on heat transfer in regular cavities filled with porous media have been done in the past decades and various extensions of the problem have been reported in the literature (see Baytas and Pop [8,9], and Baytas et al. [10]). However, it is necessary to study the heat transfer for more complex geometries because the prediction of heat transfer for irregular surfaces is a topic of great importance and irregular surfaces often occur in many applications. Recently, several studies by Rathish Kumar et al. [11,12], Murthy et al. [13] and Kumar and Shalini [14] have been reported that were concerned with the steady natural convection heat transfer in wavy vertical porous enclosures. Attachment of baffles fins or other suitable protrusion to the hot surface of fluid saturated porous enclosure can affect considerably the convection process in the system (see Riley [15]). Recently, Mahmud et al. [16], and Das and Mahmud [17] have studied the steady free convection inside vertical opposite-phase wavy enclosures and horizontal inphase wavy cavity (Benard convection problem) filled with a clean (Newtonian) fluid. Also, Mahmud and Fraser [18] reported numerical results for flow and heat transfer characteristics of a viscous and incompressible fluid (clean fluid) inside a bent cavity made of two straight-horizontal adiabatic walls and two bent-vertical isothermal walls. Rate of heat transfer in terms of local and average Nusselt numbers were calculated for different Rayleigh numbers. The prediction of fluid flow and heat transfer from irregular surface is also an important topic of aerospace application. Kubota and Uchida [19] analysed the characteristics of a transpiration cooling system with use of porous media for hypersonic reentry vehicles.

The aim of this paper is to examine the steady free convection inside a bent cavity filled with a porous medium made of two horizontal straight adiabatic walls and two bent-vertical wavy walls, which are at constant but different temperatures. The model considered is the extension of Mahmud and Fraser [18] problem to the porous medium case. However, to our best knowledge, such an investigation for a porous cavity has not been reported to date. The numerical results have been obtained numerically by solving the governing evolutionary Darcy and energy equations using the Galerkin Finite Element Method (FEM) described in the book by Zienkiewicz and Taylor [20] for a range values of the parameters like the aspect ratio (A), surface waviness (λ) and the modified Rayleigh number for the porous medium (Ra). Results are presented in terms of local and average Nusselt numbers, isotherms and streamlines for different values of the governing parameters.

2. Governing equations

The geometry of this problem as schematically shown in Fig. 1 is a porous cavity with two bent-vertical wavy walls of height L, interval spacing W and amplitude of the wavy bent wall a. It is assumed that initially the

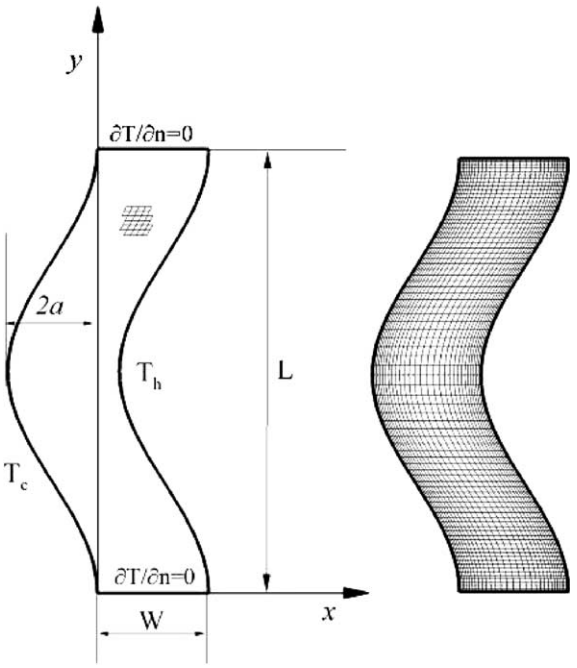

Fig. 1. Cavity geometry, boundary conditions and the grid structure.

fluid-saturated porous medium is at the constant temperature T_0 and is isothermally heated and cooled by the right and left walls at uniform temperatures T_h and T_c ($<T_h$), while the horizontal walls are adiabatic. We assume also that the flow is described by the Darcy law and that the Boussinesq approximation is used to characterize the buoyancy effect. The viscous drag and inertia terms in the governing equations are neglected, which are valid assumptions for low Darcy and particle Reynolds numbers. With these descriptions and assumptions of the problem, the governing equations are

$$\frac{\partial \bar{u}}{\partial \bar{x}}+\frac{\partial \bar{v}}{\partial \bar{y}}=0 \tag{1}$$

$$\frac{\partial \bar{u}}{\partial \bar{y}}-\frac{\partial \bar{v}}{\partial \bar{x}}=-\frac{gK\beta}{\upsilon}\frac{\partial T}{\partial \bar{x}} \tag{2}$$

$$\sigma\frac{\partial T}{\partial \bar{t}}+\bar{u}\frac{\partial T}{\partial \bar{x}}+\bar{v}\frac{\partial T}{\partial \bar{y}}=\alpha_m\left(\frac{\partial T}{\partial \bar{x}^2}+\frac{\partial T}{\partial \bar{y}^2}\right) \tag{3}$$

where $\bar{u}$ and $\bar{v}$ are the velocity components along $\bar{x}$ - and $\bar{y}$ - axes, $\bar{t}$ is the time, T is the fluid temperature and the physical meaning of the other quantities are mentioned in the Nomenclature. We introduce now the following non-dimensional variables

$$\begin{aligned} &x=\bar{x}/L, \quad y=\bar{y}/L, \quad t=(\alpha_m/\sigma L^2)\bar{t},\\ &u=(L/\alpha_m)\bar{u}, \quad v=(L/\alpha_m)\bar{v}\\ &\theta=(T-T_0)/(T_h-T_c) \end{aligned} \tag{4}$$

where $T_0=(T_h+T_c)/2$ is the characteristic temperature of the fluid-saturated porous medium. Further, we introduce the stream function, ψ, defined in the usual way as

$$u=\frac{\partial \psi}{\partial y}, \quad v=-\frac{\partial \psi}{\partial x} \tag{5}$$

so that Eqs. (2) and (3) become

$$\frac{\partial^2\psi}{\partial y^2}+\frac{\partial^2\psi}{\partial x^2}=-Ra\frac{\partial \theta}{\partial x} \tag{6}$$

$$\frac{\partial \theta}{\partial t}+\frac{\partial \psi}{\partial y}\frac{\partial \theta}{\partial x}-\frac{\partial \psi}{\partial x}\frac{\partial \theta}{\partial y}=\frac{\partial^2\theta}{\partial x^2}+\frac{\partial^2\theta}{\partial y^2} \tag{7}$$

where Ra is the Rayleigh number which is defined as

$$Ra=gK\beta(T_h-T_c)L/\alpha_m\nu \tag{8}$$

It is assumed that the wavy walls follow a profile of cosine curve. Thus, the initial and boundary conditions of these equations are

$$\begin{aligned} &t\leqslant 0: \quad \psi=\theta=0\\ &t>0: \quad \psi=0, \quad \frac{\partial\theta}{\partial n}=0 \ \text{ on } \ y=0, \quad 0\leqslant x\leqslant 1\\ &\qquad \psi=0, \quad \frac{\partial\theta}{\partial n}=0 \ \text{ on } \ y=A, \quad 0\leqslant x\leqslant 1\\ &\qquad \psi=0, \quad \theta=-1/2 \ \text{ on } \ 0\leqslant y\leqslant A,\\ &\qquad\quad x=\lambda[1-\cos(2\pi y/A)]\\ &\qquad \psi=0, \quad \theta=+1/2 \ \text{ on } \ 0\leqslant y\leqslant A,\\ &\qquad\quad x=1+\lambda[1-\cos(2\pi y/A)] \end{aligned} \tag{9}$$

where $A=L/W$ is the aspect ratio and $\lambda=a/W$ is the surface waviness of the wavy cavity.

3. Numerical formulation

Eqs. (6) and (7) subject to the initial and boundary conditions (9) are solved numerically using Galerkin Finite Element Method (FEM) described in the book by Zienkiewicz and Taylor [20]. By using FEM, the equations can be cast onto arbitrary domains without any need for the conformal transformation of the solution domain, see Fig. 1. Therefore, porous medium flow problems inside complex geometries can easily be solved. Following the method described in [20], the weak formulation of these equations can be written on two-dimensional domain, Ω, as

$$\int_\Omega\left(\frac{\partial^2\psi}{\partial x^2}+\frac{\partial^2\psi}{\partial y^2}\right)N\mathrm{d}\Omega=\int_\Omega\left(-Ra\frac{\partial\theta}{\partial x}\right)N\mathrm{d}\Omega \tag{10}$$

$$\begin{aligned} &\int_\Omega\int_t\left(\frac{\partial\theta}{\partial t}+\frac{\partial\psi}{\partial y}\frac{\partial\theta}{\partial x}-\frac{\partial\psi}{\partial x}\frac{\partial\theta}{\partial y}\right)N\mathrm{d}\Omega\mathrm{d}t\\ &\quad=\int_\Omega\int_t\left(\frac{\partial^2\theta}{\partial x^2}+\frac{\partial^2\theta}{\partial y^2}\right)N\mathrm{d}\Omega\mathrm{d}t \end{aligned} \tag{11}$$

where N is arbitrary weighting function. The spatial discretization of Eqs. (10) and (11) gives following matrix equations for the first order explicit time marching:

$$\mathbf{B}\psi = -Ra\mathbf{E}\theta \tag{12}$$

$$\mathbf{M}\theta^{n+1} = \mathbf{M}\theta^{n} - \Delta t(\mathbf{B}+\mathbf{D})\theta^{n} \tag{13}$$

where $\mathbf{B}$ is the element stiffness matrix, $\mathbf{M}$ is the lumped mass matrix, $\mathbf{D}$ is the advection matrix. $\mathbf{E}$ is the matrix for the derivatives of weighting functions. Here the superscripts "n" and "$n+1$" stand for the variable values at time levels "t" and "$t+\Delta t$". These matrices are calculated on elements, which are four-node quadrilaterals with bilinear shape functions, as:

$$\mathbf{M}_{ij} = \int_{\Omega} N_i N_j \mathrm{d}\Omega_{\mathrm{e}} \tag{14}$$

$$\mathbf{B}^{n}_{ij} = \int_{\Omega} \frac{\partial N_i}{\partial x_{\mathrm{p}}} \frac{\partial N_j}{\partial x_{\mathrm{p}}} \mathrm{d}\Omega_{\mathrm{e}} \tag{15}$$

$$\mathbf{D}^{n}_{ij} = \int_{\Omega} N_i \frac{\partial N_j}{\partial x_{\mathrm{p}}} N_k u^{n}_{k} d\Omega_{\mathrm{e}} + \int_{\Omega} N_i \frac{\partial N_j}{\partial x_{\mathrm{p}}} N_k v^{n}_{k} \mathrm{d}\Omega_{\mathrm{e}} \tag{16}$$

$$\mathbf{E}_{\alpha i} = \int_{\Omega} N_i \frac{\partial N_i}{\partial x_{\alpha}} \mathrm{d}\Omega_{\mathrm{e}} \tag{17}$$

here u and v are defined by Eq. (5). The Poisson equation for stream function, ψ, is solved using Element-by-Element Iteration technique with Conjugate Gradient Method. This technique does not require assembly of the element stiffness matrices to obtain global stiffness matrix. Therefore it saves the storage of the memory and execution time. The details of this method can be found in Gulcat [21].

The physical quantities of interest are the local Nusselt number, Nu, which is calculated at the walls as

$$Nu = \left.\frac{\partial\theta}{\partial n}\right|_{\mathrm{wall}} \tag{18}$$

and the average Nusselt number, Nu_{a}, which is obtained by integration of local Nusselt numbers over the walls as

$$Nu_{\mathrm{a}} = \frac{1}{S}\int_{0}^{S} Nu\,\mathrm{d}s \tag{19}$$

Here S is the length of the wall where the Nusselt number is evaluated.

To check if the steady state solution is obtained or not, the variation of stream function and temperature distribution is observed between the consecutive time steps according to following equation

$$\sum \left|\varphi^{n+1}_{i,j} - \varphi^{n}_{i,j}\right| \Big/ \sum \left|\varphi^{n+1}_{i,j}\right| \leqslant \varepsilon \tag{20}$$

where φ stands for both temperature and stream function, ε is the prescribed error, which is 10^{-5}, at time level $n+1$.

4. Results and discussions

Various computations were carried out for the following ranges: The Rayleigh number, Ra, from 10 to 10^3, the aspect ratio, A, 1–5 and surface waviness, λ, from 0 (plane walls) to 0.6. The results are given to carry out a parametric study showing influences of several of these non-dimensional parameters. The finite element grid for the results presented in the following pages contains 2400 elements and 2511 nodes, where there are 31 points along the width of the cavity and 81 points along the height. Time step size is dictated by the stability criteria, as given in Gulcat [21], which is taken as $\Delta t = 1\times10^{-5}$. For the validation of the numerical method used in this study, a square cavity ($A = 1$) with plane walls ($\lambda = 0$) at the steady-state flow is solved. For this problem, the values of Nu_{a} on the vertical walls are given in Table 1; the grid considered being 45×45. It is seen that the present values of Nu_{a} are in very good agreement with those obtained by different authors, such as Walker and Homsy [22], Bejan [23], Beckerman et al. [24], Gross et al. [25], Manole and Lage [26], Moya et al. [27], and Baytas and Pop [28]. Therefore, it can be concluded that the developed code can be used with great confidence to study the problem discussed in this paper.

The typical temperature and flow fields are shown in Figs. 2–9 (isotherms are on the top and streamlines on the bottom). It is seen from these figures that as for cavities filled with a porous medium with plane walls or cavities with bent-vertical walls filled with a clear fluid (see, Mahmud and Fraser [18]) hot fluid moves up along the hot wall (right) and turns to the cold wall (left) at the top adiabatic wall and then mixes with the stream of downward-moving cold fluid along the cold wall. This causes the circulation inside the cavity which is very weak in strength at low Rayleigh number (=10). Isothermal lines nearly follow the geometry of the wavy surface and it gives a clear indication of a conduction-dominant flow and heat transfer. It is also seen that the results for $A = 1$ and 2 with $\lambda = 0.5$, shown in Figs. 2 and 3, indicate the convection mainly occurs within the hot wall.

Table 1
Comparison of the average Nusselt number at different values of Ra for $A = 1$ (square cavity) and $\lambda = 0$ (plane vertical walls)

Authors	$Ra = 10^1$	$Ra = 10^2$	$Ra = 10^3$
Walker and Homsy [22]		3.097	12.96
Bejan [23]		4.2	15.8
Beckerman et al. [24]		3.113	
Gross et al. [25]		3.141	13.448
Manolo and Lage [26]		3.118	13.637
Moya et al. [27]	1.065	2.801	
Baytas and Pop [28]	1.079	3.16	14.06
Present study	1.119	3.05	13.15

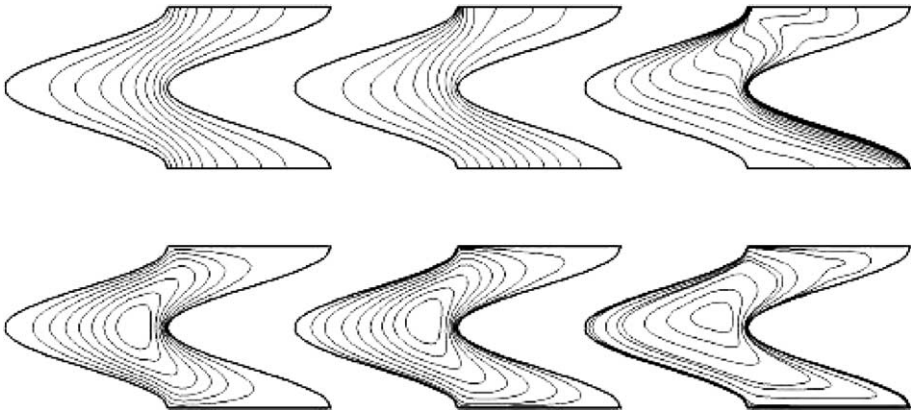

Fig. 2. Isotherms (top) and streamlines (bottom) for $A = 1$, $\lambda = 0.5$, at $Ra = 10, 100, 1000$ (left to right).

This is because the temperature difference between the right wall and the porous medium is larger (positive) than that between the left wall and the porous medium. Further, Figs. 2–9 show that for all values of the parameters considered the flow is one egg cell, except for $Ra = 10$, $A = 4$ and $\lambda = 0.6$ in Fig. 7 where there exist two egg shaped cells, one at the adiabatic top wall and the other in the middle of the cavity dividing it into two flow portions. This type of flow pattern is absent in a cavity with vertical straight walls ($\lambda = 0$) at low Rayleigh number. Further increase of the Rayleigh number increases the strength of the circulation inside the cavity as can be seen from Figs. 2–6 At $Ra = 10^3$, thermal boundary layers are formed in the vicinity of the wavy walls and the isothermal lines are highly concentrated at these walls. The development of thermal boundary layers greatly intensifies the isotherm as well as temperature gradient in the vicinity of the wavy walls.

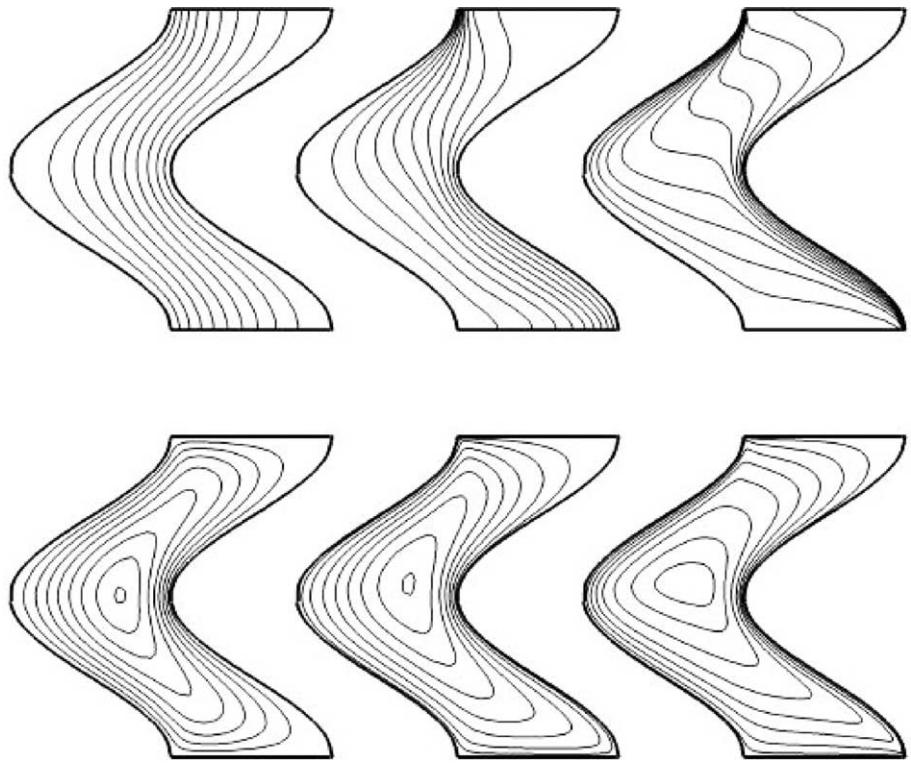

Fig. 3. Isotherms (top) and streamlines (bottom) for $A = 2$, $\lambda = 0.5$, at $Ra = 10, 100, 1000$ (left to right).

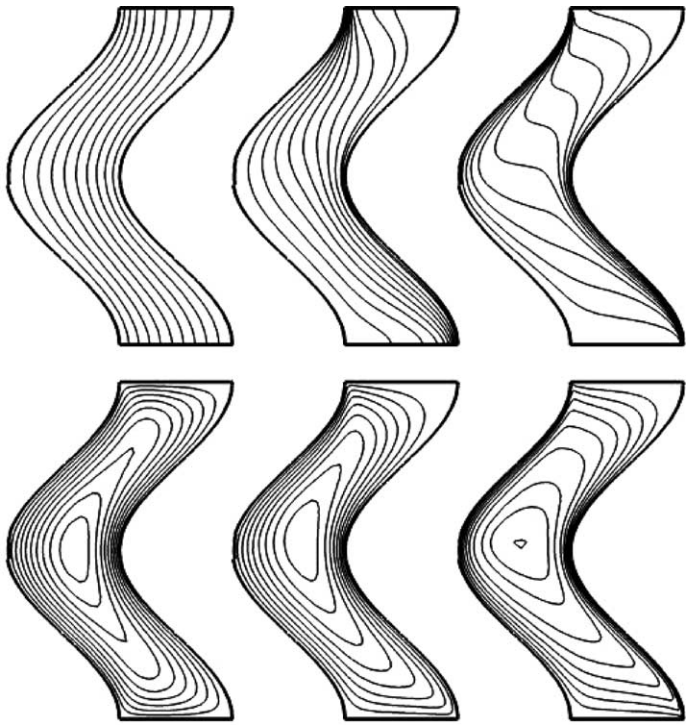

Fig. 4. Isotherms (top) and streamlines (bottom) for $A = 3$, $\lambda = 0.5$, at $Ra = 10$, 100, 1000 (left to right).

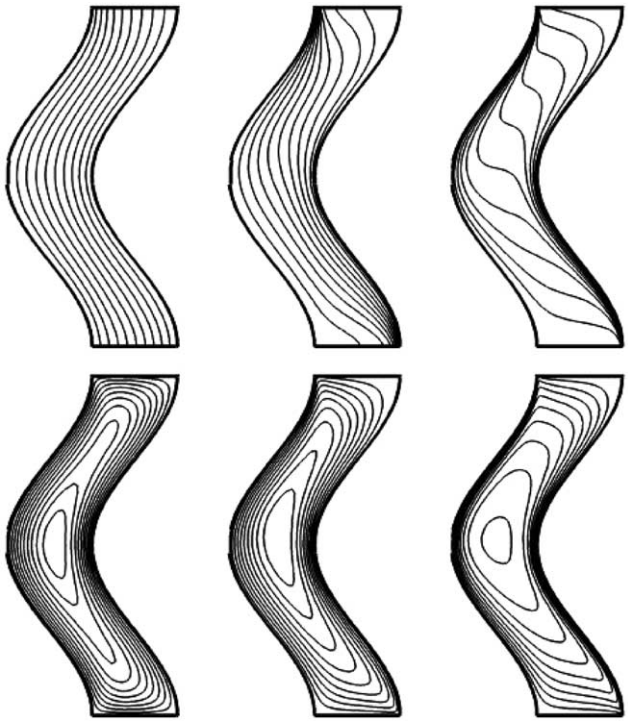

Fig. 5. Isotherms (top) and streamlines (bottom) for $A = 4$, $\lambda = 0.5$, at $Ra = 10$, 100, 1000 (left to right).

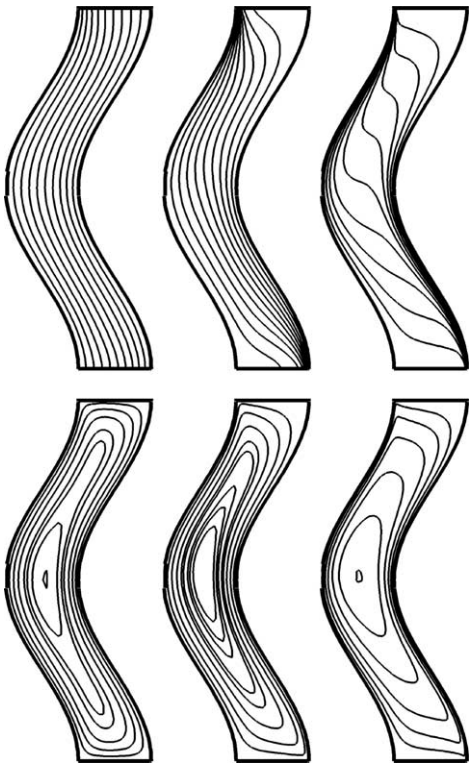

Fig. 6. Isotherms (top) and streamlines (bottom) for $A = 5$, $\lambda = 0.5$, at $Ra = 10$, 100, 1000 (left to right).

Further, Table 2 shows the values of the average Nusselt number Nu_a at the hot bent-wall (right wall) of the cavity for different aspect ratios A and wave amplitude λ. One can see from this table that Nu_a increases with the increase of Ra for all values of A and λ considered. However, the values of Nu_a increases monotonically with the increase of both Ra and A for small values of λ(=0.4). For $A = 4$ and $\lambda = 0.3$, the values of Nu_a are higher than those for other values of λ considered. This behaviour may be explained in connection with different flow regimes inside the porous cavity, namely, conduction and critical regimes, respectively, as termed by Mahmud and Fraser [18].

Finally, Figs. 10 and 11 illustrate the variation of the local Nusselt number, Nu with the non-dimensional coordinate y along the vertical hot and cold walls, respectively, for some values of A and λ when $Ra = 1000$. It is seen from Fig. 10 that for the hot wall, the values of Nu are higher for $A = 5$ (a large cavity ratio) than for $A < 5$ (moderate cavity ratio) when λ (=0.5) is fixed. It is also seen, that for $A > 3$, Nusselt number remains positive at any distance from the lower horizontal wall (any value of y), i.e. heat is transferred in the negative x direction. For cavities with $A = 1$, 2 and 3, on the other hand, the situation becomes quite different. In this case, Nusselt number may even become negative for the both cold and hot walls of the cavity for some values of y. This is due essentially to the geometry of the wavy

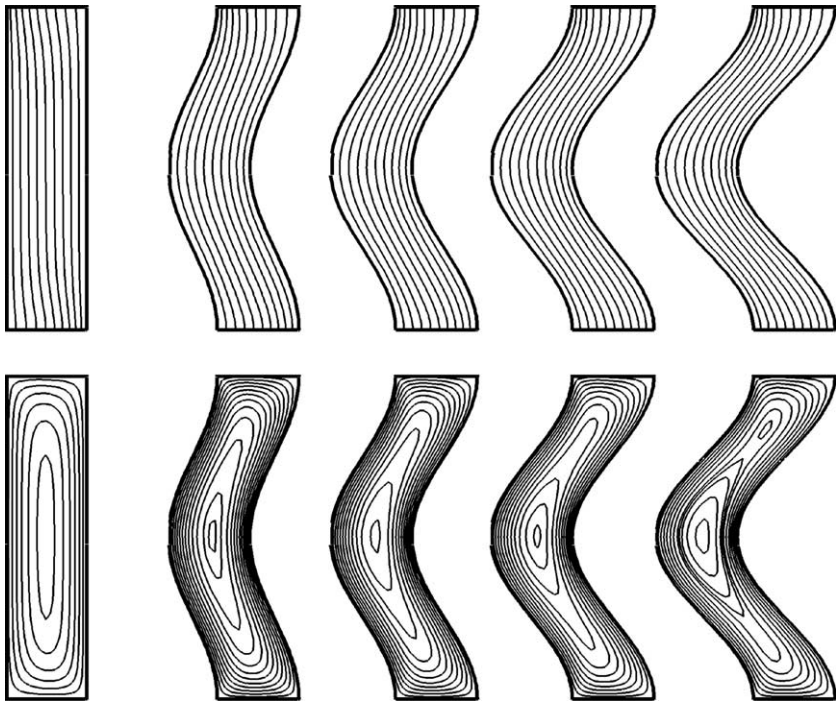

Fig. 7. Isotherms (top) and streamlines (bottom) at $Ra = 10$ for $A = 4$ and $\lambda = 0$, 0.3, 0.4, 0.5, 0.6 (left to right).

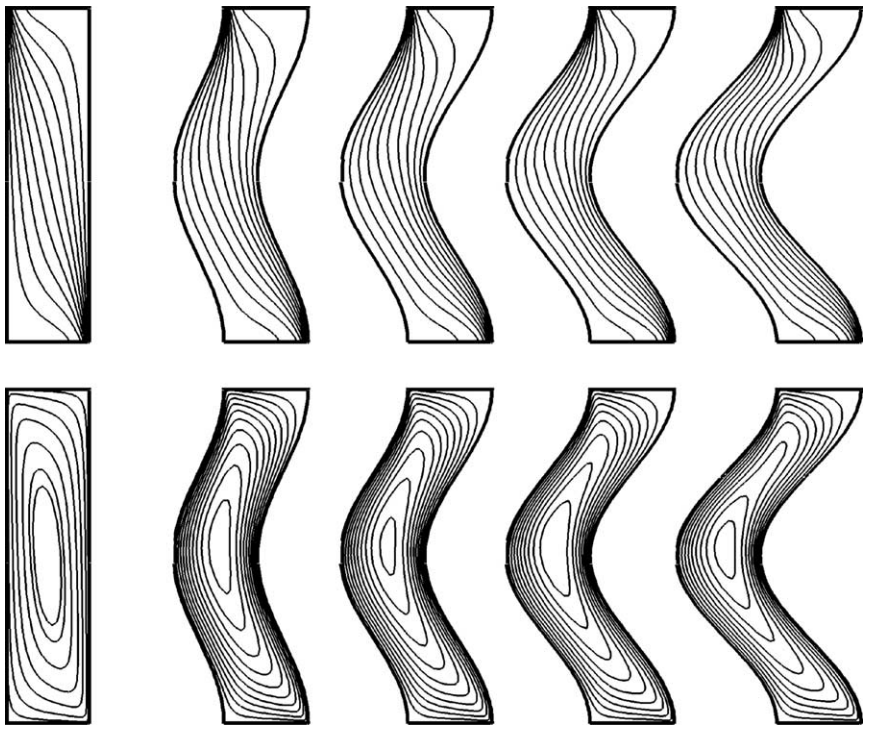

Fig. 8. Isotherms (top) and streamlines (bottom) at $Ra = 100$ for $A = 4$ and $\lambda = 0$, 0.3, 0.4, 0.5, 0.6 (left to right).

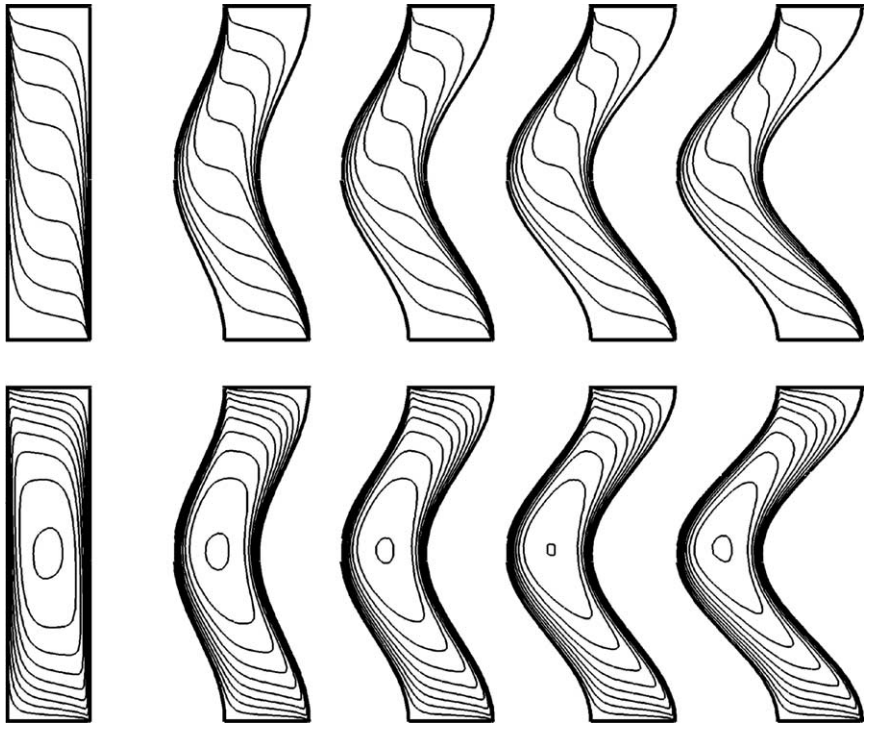

Fig. 9. Isotherms (top) and streamlines (bottom) at $Ra = 1000$ for $A = 4$ and $\lambda = 0$, 0.3, 0.4, 0.5, 0.6 (left to right).

Table 2
Values of the average Nusselt number at the hot bent-wall for different aspect ratios and wave amplitude

		Nusselt number for hot wall		
		$Ra = 10^1$	$Ra = 10^2$	$Ra = 10^3$
$A = 4$	$\lambda = 0$	1.077	2.215	7.339
	$\lambda = 0.3$	1.079	2.303	7.884
	$\lambda = 0.4$	1.072	2.236	7.768
	$\lambda = 0.5$	1.064	2.139	7.551
	$\lambda = 0.6$	1.055	2.024	7.264
$\lambda = 0.5$	$A = 1$	0.893	1.368	5.803
	$A = 2$	0.980	2.213	8.044
	$A = 3$	1.041	2.260	8.038
	$A = 4$	1.064	2.139	7.551
	$A = 5$	1.073	1.993	7.015

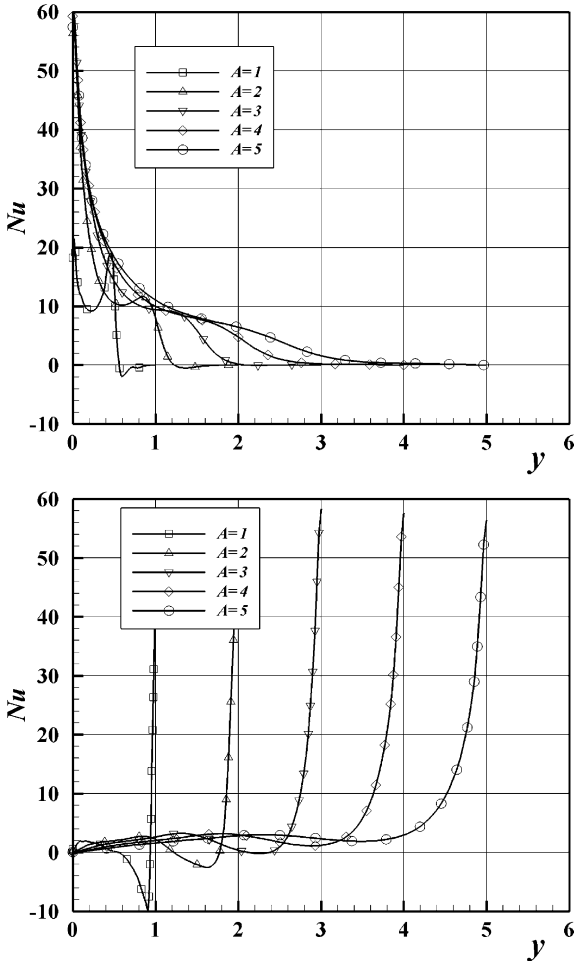

Fig. 10. Variation of local Nusselt number along the hot (above) and cold (below) walls at $Ra = 1000$ and $= 0.5$ for different values of A.

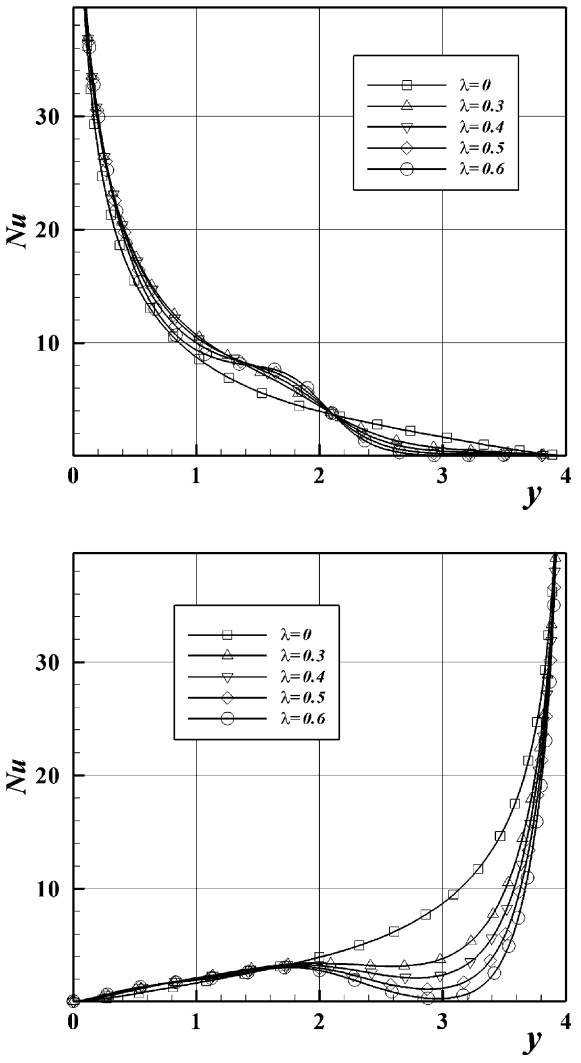

Fig. 11. Variation of local Nusselt number along the hot (above) and cold (below) walls at $Ra = 1000$ and $A = 4$ for different values of λ.

wall. The measure of local heat transfer depends on the slope of the wavy wall, and the local heat transfer is managed by the fluid flow influenced by the buoyancy force parallel to the wavy surface. For the lower portion of the hot wavy surface, the velocity is larger and so is the heat transfer rate. Convection-favouring buoyancy forces are relatively larger along the lower portion of the hot wavy surface then the upper portion of the hot wavy wall. It means for the hot wall that the energy produced in the porous medium cannot be transferred out from the right (hot) wall, while the right wall at higher temperature will transfer heat towards the left wall at lower temperatures. This principle can applies also for the case of the cold wall as follows. The velocity and the local heat transfer rate are larger on the upper por-

tion of the cold wavy surface. The convection heat transfer is dominant on this portion of the wavy wall. The fluid flow is held on the lower half part of cold wavy surface protruding out of the domain. For this reason, the velocity and the local heat transfer rate are not larger on the convex portion of the lower cold wall. However, at $A = 1$ the value of Nusselt number is at its lowest negative value. Then it increases and remains constant and positive. The constant values of Nusselt number also take place for $A > 1$ and large values of y. The reason for the extreme negative Nusselt number to occur at $A = 1$ may be due to an intensive convection in the square bent cavity.

Fig. 11 indicates that values of Nusselt number are positive for both hot and cold walls when $A = 4$ and all values of λ considered. This can be explained due to the fact that contribution of conduction becomes more dominant at large aspect ratio values.

5. Conclusions

The steady natural convection inside a cavity made of two horizontal straight walls and two vertical wavy walls which follow a profile of cosine curve and filled with a fluid-saturated porous medium has been numerically examined in this paper. The governing equations were solved using the Galerkin Finite Element Method (FEM), which is one of the most commonly known methods for such problems (Zienkiewicz and Taylor [20]). The results are presented in terms of the isotherms and stream functions and local and average Nusselt numbers from the bent-vertical walls. The comparison of the present results for a cavity with plane vertical walls ($\lambda = 0$) with those reported in the open literature are very good. The study indicates that for large values of the Rayleigh number, Ra (=1000), and moderate values of the aspect ratio A (smaller than 3) and of the surface waviness, λ (=0.5), the local Nusselt number from the vertical walls may even become negative; this means the heat generated in the porous medium cannot be transferred through the porous medium from the right (hot) wall to the left (cold) wall.

References

[1] D.B. Ingham, I. Pop (Eds.), Transport Phenomena in Porous Media, vol. II, Pergamon, Oxford, 2002.

[2] D.A. Nield, A. Bejan, Convection in Porous Media, second ed., Springer, New York, 1999.

[3] K. Vafai (Ed.), Handbook of Porous Media, vol. II, Marcel Dekker, New York, 2004.

[4] I. Pop, D.B. Ingham, Convective Heat Transfer: Mathematical and Computational Modelling of Viscous Fluids and Porous Media, Pergamon, Oxford, 2001.

[5] A. Bejan, A.D. Kraus (Eds.), Heat Transfer Handbook, Wiley, New York, 2003.

[6] D.B. Ingham, A. Bejan, E. Mamut, I. Pop (Eds.), Emerging Technologies and Techniques in Porous Media, Kluwer, Dordrecht, 2004.

[7] A. Bejan, I. Dincer, S. Lorente, A.F. Miguel, A.H. Reis (Eds.), Porous and Complex Flow Structures in Modern Technologies, Springer, New York, 2004.

[8] A.C. Baytas, I. Pop, Natural convection in a trapezoidal enclosure filled with a porous medium, Int. J. Engng. Sci. 39 (2001) 125–134.

[9] A.C. Baytas, I. Pop, Free convection in a square porous cavity using thermal non-equilibrium model, Int. J. Thermal Sci. 41 (2002) 861–870.

[10] A.C. Baytas, A. Filiz Baytas, I. Pop, Free convection in a porous cavity filled with pure or saline water, in: ICAPM 2004, A.H. Reis, A.F. Miguel, (Eds.), Applications of Porous Media, May 24–27, Evora, Portugal, 121–125.

[11] B.V. Ratish Kumar, P. Singh, P.V.S.N. Murthy, Effect of surface undulations on natural convection in a porous square cavity, ASME J. Heat Transfer 119 (1997) 848–851.

[12] B.V. Ratish Kumar, P.V.S.N. Murthy, P. Singh, Free convection heat transfer from an isothermal wavy surface in a porous enclosure, Int. J. Numer. Meth. Fluids 28 (1998) 633–661.

[13] P.V.S.N. Murthy, B.V. Rathish Kumar, P. Singh, Natural convection heat transfer from a horizontal wavy surface in a porous enclosure, Numer. Heat Transfer Part A 31 (1997) 207–221.

[14] B.V. Rathish Kumar, Shalini, Free convection in a non-Darcian wavy porous enclosure, Int. J. Engng. Sci. 41 (2003) 1827–1848.

[15] D.S. Riley, Steady two-dimensional thermal convection in a vertical porous slot with spatially periodic boundary imperfections, Int. J. Heat Mass Transfer 31 (1988) 2365–2380.

[16] S. Mahmud, P.K. Das, N. Hyder, A.K.M.S. Islam, Free convection in an enclosure with vertical wavy walls, Int. J. Therm. Sci. 41 (2002) 440–446.

[17] P.K. Das, S. Mahmud, Numerical investigation of natural convection inside a wavy enclosure, Int. J. Therm. Sci. 42 (2003) 397–406.

[18] S. Mahmud, R.D. Fraser, Free convection and entropy generation inside a vertical inphase wavy cavity, Int. Commun. Heat Mass Transfer 31 (2004) 455–466.

[19] H. Kubota, S. Uchida, Thermal protection system with use of porous media for a hypersonic reentry vehicle, J. Porous Med. 2 (1999) 71–86.

[20] O.C. Zienkiewicz, R.L. Taylor, The Finite Element Method, vol. I, McGraw-Hill Book Company, London, 1989.

[21] U. Gulcat, An explicit FEM for 3-D general viscous flow studies based on EBE/PCG iterative algorithm, Comp. Fluid Dyn. 4 (1995) 73–85.

[22] K.L. Walker, G.M. Homsy, Convection in a porous cavity, J. Fluid Mech. 97 (1978) 449–474.

[23] A. Bejan, On the boundary layer regime in a vertical enclosure filled with a porous medium, Lett. Heat Mass Transfer 6 (1979) 93–102.

[24] C. Bekermann, R. Viskanta, S. Ramadhyani, A numerical study of non-Darcian natural convection in a vertical enclosure filled with a porous medium, Numer. Heat Transfer Part A 10 (1986) 557–570.

[25] R.J. Gross, M.R. Bear, C.E. Hickox, The application of flux-corrected transport (FCT) to high Rayleigh number

natural convection in a porous medium, in: Proceedings of 8th International Heat Transfer Conference, San Francisco, CA, 1986.

[26] D.M. Manole and J.L. Lage, Numerical benchmark results for natural convection in a porous medium cavity, in: Heat and Mass Transfer in Porous Media, ASME Conference, HTD 216 (1992) 55–60.

[27] S.L. Moya, E. Ramos, M. Sen, Numerical study of natural convection in a tilted rectangular porous material, Int. J. Heat Mass Transfer 30 (1987) 741–756.

[28] A.C. Baytas, I. Pop, Free convection in oblique enclosures filled with a porous medium, Int. J. Heat Mass Transfer 42 (1999) 1047–1057.